Experiment 6: Geometric Optics

Naim Ayat: 104733125

16 November 2017

Thursday 11:00AM PST

David Bauer

Lab Partner: Adam Jankowski

6.4.1 Worksheet

1. (a) The critical angle for the fiber-cladding interface β_c is modeled by:

$$\beta_c = sin^{-1}\frac{n_{clad}}{n_{fiber}}. \quad (1)$$

From the given values $n_{clad} = 1.4$ and $n_{fiber} = 1.5$, we calculate that $\beta_c = 1.2\,rad$ by equation (1).

(b) By the definition of complimentary angles, we know that $\alpha + \beta = \frac{\pi}{2}\,rad$. We also know that the condition for total internal reflection (TIR) is $\beta > critical\ angle$. In our case, therefore, the critical angle is $1.2\,rad$. Note that where β is at its minimum value $1.2\,rad$, the maximum value of α is $0.371\,rad$. It follows that, to maximize β, the minimum value of α is $0\,rad$ (non-inclusive, because $\alpha = 0$ implies no reflection). Hence, $0\,rad < \alpha \leq 0.371\,rad$.

(c) Snell's law allows us to determine the range of incident angles θ wherein the light experiences TIR at the fiber-cladding interface. The law is defined as:

$$n_{air}\sin(\theta) = n_f \sin(\alpha). \quad (2)$$

Using the fact that α is in the range $(0\,rad, 0.371\,rad]$, we solve for θ in equation (2). This calculation yields the range $0\,rad < \theta \leq 0.575\,rad$.

(d) If the light undergoes TIR on the first bounce (at the point with angle β), this implies that the light will continue to bounce down the fiber interface of the cable. Depending on adjustments to cable orientation and relevant angles, the light may leave the interface later in its propagation.

2. The critical angle is the first angle where TIR occurs and possesses the special property that refraction is at 90° from the normal vector. Thus, it differs from any general TIR angle.
3. Snell's law is given by:

$$n_i \sin(\theta_i) = n_t \sin(\theta_t). \quad (3)$$

where n_t represents the index of refraction for the material transmitted through the prism, n_i represents the index of refraction for air, θ_i is the angle in, and θ_t is the transmitted angle. From our lab, the rays into the system are defined by $(0.4887 \pm 0.0004)\,rad$. The rays transmitted are defined by $(0.2967 \pm 0.0004)\,rad$. We use equation (3) with these

rays and the index of refraction for air in a vacuum, $n_i = 1$, to determine the index of refraction for the prism n_{prism}. The error of this calculation is given by:

$$\delta n_{prism} = \sqrt{\left(\frac{n_i \delta\theta_i \cos(\theta_i)}{\sin(\theta_t)}\right)^2 + \left(\frac{-(n_i \delta\theta_t \sin(\theta_i)\cos(\theta_t))}{sin^2(\theta_t)}\right)^2}. \quad (4)$$

From equations (3) and (4), we determine that $n_{prism} = (1.606 + 0.002)$. We can find the critical angle θ_c and its error with the following formulae:

$$\theta_c = sin^{-1}\left(\frac{n_i}{n_{prism}}\right) \quad \text{and} \quad (5)$$

$$\delta\theta_c = \frac{-\delta n_{prism} n_i}{n_{prism}^2 \sqrt{1-\left(\frac{n_i}{n_{prism}}\right)^2}}. \quad (6)$$

From equations (4) and (5), we calculate $\theta_c = (0.68 \pm 0.05)\, rad$. Meanwhile, our measured value for the critical angle is $\theta_c = (0.7069 \pm 0.0004)\, rad$. We can determine the percent error associated with our measured value with the formula:

$$\%\, error = \left|\frac{measured - calculated}{calculated}\right| * 100. \quad (7)$$

Hence, we find that the measured value has 3.9% error by equation (7). We also note that the measured value falls within the uncertainty of the calculated value; thus, our measured critical angle corroborates our value for n_{prism}.

4. The equation for addition of thin lens focal lengths with finite separation is:

$$\frac{1}{f_{total}} = \frac{1}{f_1} + \frac{1}{f_2} - \frac{e}{f_1 f_2} \quad (8)$$

where e represents the distance between lenses. Hence, $f_{total} \to \infty$ when $e = f_1 + f_2$. As f_{total} increases without bound, the beams through the second lens do not converge or diverge; rather, they must be parallel. This configuration is displayed in Fig. (1) below.

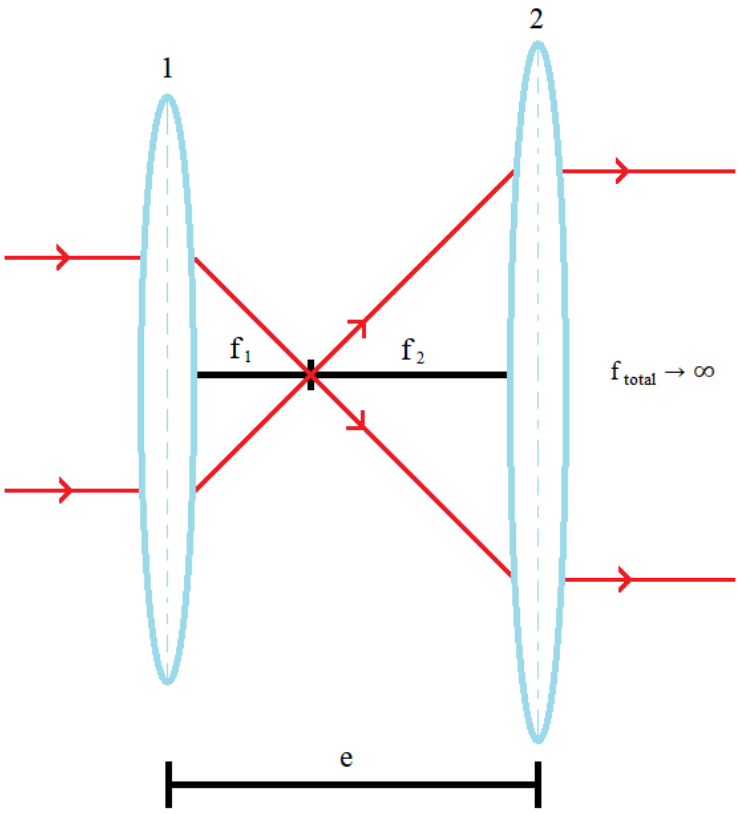

Figure 1: Demonstrating infinite effective focal length over thin lenses. Two thin lenses, labeled (1) and (2), have respective focal lengths f_1 and f_2. When the distance between them is $e = f_1+f_2$, the effective focal length is modeled by $f_{total} \to \infty$. This configuration of lenses can be employed to extend the length of parallel beams.

6.4.2 Presentation Report

2. Introduction

This experiment serves to examine some of the geometric and physical characteristics demonstrated by light rays propagating through thick and thin lenses.

With a ray box and baffle, we will arrange three parallel rays of light to propagate through a bi-convex lens, a bi-concave lens, and a plano-convex lens. For each lens, we will position the lens at a distance from the ray box and trace the intersection of the rays to find the focal length. Then, using five rays from the ray box, we will demonstrate spherical aberration resulting from the bi-convex lens. To observe 1D magnification, we will generate three diverging rays with the bi-concave lens, then parallelize them with the plano-convex lens. We may then calculate the magnification factor M:

$$M = \frac{separation_{final}}{separation_{initial}}. \tag{9}$$

Next, we will propagate a laser through a beam splitter such that two parallel beams are generated about $1\ cm$ apart from each other. The beams will shine through a thin lens with a diameter of $3.5\ cm$. Upon measuring the distances at which the beams converge and diverge, we will be able to calculate the focal length f. With this information, we repeat this process for a smaller thin lens and calculate the dioptric power P for each of the two thin lenses:

$$P = \frac{1}{f}. \tag{10}$$

Further, we will measure the focal length and dioptric power of the two lenses in series to confirm that dioptric power is additive.

We will measure the focal length of a ball lens and compare it to the theoretical model:

$$f_{ball} = \frac{nD}{4(n-1)} \tag{11}$$

where n is refractive index and D is diameter.

Finally, we will propagate an LED light though a mesh surface (with $1\ mm$ gaps) and a $2\ cm$ diameter thin lens. The distance of the object from the lens will be varied such that we can determine where the image is clear and real. We seek to generate results that agree with the Lens Maker's formula:

$$\frac{1}{f} = \frac{1}{o} + \frac{1}{i}. \tag{12}$$

where o is the distance between the object and the lens and i is the distance between the lens and the image. We will also measure the distance of grating on the image and determine whether our measurements agree with the theoretical model:

$$\frac{I}{O} = \frac{i}{o} = \frac{f}{o-f} \tag{13}$$

where O is the magnitude of grating on the object and I is the grating spacing on the image.

3. Experimental Results

Using a ray box, we propagate a ray which is split into three with a baffle. The ray box is placed at a distance away from one of three thick lenses (bi-concave, bi-convex, and plano-convex). We measure the distance between the center of the lens and the point at which the rays intersect. We repeat this for the two remaining thick lenses. From this information, we determine that the bi-concave thick lens has a focal length of $-0.0390 \pm 0.0005\ m$, the bi-convex thick lens has a focal length of $0.0580 \pm 0.0005\ m$, and the plano-convex thick lens has a focal length of $0.1050 \pm 0.0005\ m$.

Next, we set the baffle to produce five rays from the left that shine through the bi-convex lens to the right. We observe that there appear to be two additional focal lengths because of spherical aberration. We block out the three middle rays, which makes the second focal length more clearly visible. From left to right, we measure that the first focal length occurs at a distance $0.0520 \pm 0.0005\ m$ from the center of the lens and the last occurs at a distance $0.0560 \pm 0.0005\ m$ from the center of the lens.

We reconfigure the baffle to produce three rays, then shine the rays through the bi-concave lens and the plano-convex lens in sequence. We vary the distance of the latter lens until we observe that the rays propagate in parallel with maximum separation between

them. Since the initial separation is measured to be $0.0100 \pm 0.0005\, m$ and the final separation is $0.0050 \pm 0.0005\, m$, the magnification factor is $M = 2.0 \pm 0.1$ by equation (9). We repeat this process such that the plano-convex lens comes before the bi-concave lens in sequence. This time, we vary the latter to observe the minimum separation between the rays. The initial separation is constant from the prior calculation and the final separation is measured to be $0.0200 \pm 0.0005\, m$. Thus, we yield a demagnification factor $M = 0.50 \pm 0.06$ by equation (9).

We configure a laser to propagate through a splitter at $45°$ from the horizontal. This generates two parallel beams at a distance of $1\ cm$ apart, which shine through a thin lens and hit a piece of paper. We vary the paper along a horizontal track and measure where the two rays converge and diverge. We find the midpoint between these two distances, which serves as the best value for the focal length of the lens. We follow this procedure with five different lenses. The results are recorded in Fig. (2).

Lens	**Focal Length, f (m)**	**Dioptric Power, P (m^{-1})**
Thin Lens (D = 3.5 cm)	0.380 ± 0.005	2.63 ± 0.03
Thin Lens (D = 2.5 cm)	0.097 ± 0.001	10.3 ± 0.1
Above thin lenses in series	0.077 ± 0.001	13.0 ± 0.2
Thin Lens (D = 2.0 cm)	0.166 ± 0.007	6.0 ± 0.3
Ball Lens (n = 1.5)	0.0180 ± 0.0007	56 ± 2

Figure 2: Measured focal lengths and calculated dioptric power for five lens configurations. The focal lengths are the distances from the center of the lenses to the center of the rays' convergence point. Uncertainties stem from the propagation of errors from a millimeter ruler. Dioptric power is the inverse of focal length as calculated by equation (10).

We arrange an LED on a horizontal track next to an object with grating such that the light can produce its image. We put the thin lens with a diameter of 2.0cm further down the track, followed by a piece of paper beyond the lens to capture the final image. We vary the lens and paper such that the image is real and clear. We find a range of values to obtain best values for o and i as per equation (12). We also measure image grating size I with a ruler. The relevant measurements are displayed in Fig. (3).

Trial #	Focal Length, f (m)	Image Distance, i (m)	Object Distance, o (m)	Image Grating Size, I (m)
1	0.166 ± 0.007	0.53 ± 0.01	0.2360 ± 0.0007	0.0025 ± 0.0005
2	0.166 ± 0.007	0.314± 0.004	0.3300 ± 0.0007	0.0009 ± 0.0001
3	0.166 ± 0.007	0.25± 0.02	0.4000 ± 0.0007	0.0005 ± 0.0001

Figure 3: Focal lengths, image distances, object distances, and image grating sizes measured over three image formation trials. All measurements are made by hand with a millimeter ruler. Thus, uncertainties stem from the propagation of error from a millimeter ruler.

3. Analysis

From the first procedure, we observed that the bi-concave lens has a negative focal length. This is to be expected, as bi-concave lenses diverge rays that pass through them. Conversely, we found that the bi-convex lens has a positive focal length, since it converges rays. Finally, the plano-convex lens has a positive focal length that is greater than that of the bi-convex lens. This is because the plan-convex lens is flat and curved only on one side; thus, it does not converge rays as quickly as the bi-convex lens.

In the spherical aberration procedure, we note that the bi-convex lens appears to generate two additional focal lengths because the two rays at the edges of the lens are refracted more than the three in the center. The focal length furthest left occurs at a distance $0.0520 \pm 0.0005\ m$ from the center of the lens and the focal length furthest right occurs at a distance $0.0560 \pm 0.0005\ m$ from the center of the lens. The midpoint, therefore, is $0.0540 \pm 0.0007\ m$ from the center of the lens when accounting for the accumulated propagation of error. Using the percent error formula (7) with $0.0540m$ as our experimental value and $0.0560m$ as our theoretical value, we calculate that spherical aberration causes our focal point to deviate by 3.6%.

For our calculation of 1D magnification with a bi-concave lens and plano-convex lens in series, we yielded $M = 2.0 \pm 0.1$ from equation (9). The uncertainty is given by:

$$\delta M = \sqrt{\left(\frac{\delta separation_{final}}{separation_{initial}}\right)^2 + \left(\frac{\delta separation_{initial} separation_{final}}{separation_{initial}^2}\right)^2}\ . \qquad (14)$$

By the same method, we calculated the demagnification associated with a plano-convex lens and a bi-convex lens in series to be $M = 0.50 \pm 0.06$. We note that these M values are inverse.

The uncertainty for dioptric power calculations in Fig. (2) is given by:

$$\delta P = P_{best} \frac{\delta f}{f}. \tag{15}$$

By the additive property of dioptric power, we expect that the theoretical dioptric power of the combination of thin lenses in Fig. (2) will be the sum of the dioptric power of the two individual lenses. Thus, the theoretical value is:

$$P_{theoretical} = (2.63 \pm 0.3)m^1 + (10.3 \pm 0.1)m^1 = (12.9 \pm 0.1)m^1 \, . \tag{16}$$

In row three of Fig. (2), we observe that the experimental dioptric power value was $(13.0 \pm 0.2)m^1$. This value has an error of 0.77% by equation (7) and falls within the uncertainty of $P_{theoretical}$. Thus, our result upholds the additive property of dioptric power.

We can determine theoretical image distance values i_t and compare them to the measured i values in Fig. (3). Note that theoretical image distance can be obtained by solving equation (13) for i. Hence:

$$i_{theoretical} = \frac{of}{o-f}. \tag{17}$$

The uncertainty is given by:

$$\delta i_{theoretical} = \sqrt{\left(-\frac{\delta o f^2}{(o-f)^2}\right)^2 + \left(\frac{\delta f^2}{(f-o)^2}\right)^2}. \tag{18}$$

We compare theoretical and measured image distance in Fig. (4).

Trial #	Theoretical Image Distance, i_t (m)	Measured Image Distance, i (m)	Percent Error
1	0.55 ± 0.08	0.53 ± 0.01	3.6%
2	0.33± 0.03	0.314± 0.004	4.8%
3	0.27± 0.03	0.25± 0.02	10.7%

Figure 4: Comparison of theoretical and measured image distances over three image formation trials. Measured image distances are taken from Fig. (3) and theoretical image distances are calculated with equations (17) and (18). We observe a maximum percent error of 10.7%; however, the measured values fall within the uncertainties of their corresponding theoretical values. Thus, our measurements uphold equation (13).

Now, we examine the measured image grating size data and compare it to the theoretical model in equation (13). Solving for I, we obtain the theoretical model:

$$I_{theoretical} = \frac{Of}{o-f} \tag{19}$$

with uncertainty given by:

$$\delta I_{theoretical} = \sqrt{\left(\frac{\delta f O o}{(f-o)^2}\right)^2 + \left(-\frac{\delta o O}{(o-f)^2}\right)^2}. \tag{20}$$

In our case, $O = 1\ mm$. From these equations, we generate a comparison of measured and theoretical image grating size in Fig. (5).

Trial #	Theoretical Image Grating, I_t (m)	Measured Image Grating, I (m)	Percent Error	Magnification
1	0.0024 ± 0.0004	0.0025 ± 0.0005	4.2%	Magnified
2	0.0008 ± 0.0003	0.0009 ± 0.0001	12.5%	Demagnified
3	0.0007 ± 0.0003	0.0005 ± 0.0001	28.6%	Demagnified

Figure 5: Comparison of theoretical and measured image grating sizes over three image formation trials. Measured image grating sizes are taken from Fig. (3) and theoretical image grating sizes are calculated with equations (19) and (20). Magnification occurs when $f < o < 2f$. Demagnification occurs when $o > 2f$. We observe a maximum percent error of 28.6%; however, the measured values fall within the uncertainties of their corresponding theoretical values. Thus, our measurements uphold equation (13).

4. Conclusion

We determined that spherical aberration caused the focal length of our bi-convex lens to deviate by 3.6%. We also observed that placing bi-concave and plano-convex lenses in series caused reciprocal magnification when the order of the lenses was swapped.

Nevertheless, our primary objective for this experiment was to obtain measured values that were consistent with the theoretical models for the examined lens properties – namely the additivity of dioptric power, Lens Maker's formula (12), and equation (13). The measured values fell within the uncertainties of their corresponding theoretical values for every case. That is – our measured dioptric power agreed with theoretical dioptric power, measured image distance agreed with theoretical image distance, and measured image grating agreed with theoretical image grating. Again, this means that all measured values fell within their corresponding theoretical uncertainties. However, we obtained percent error values as high as 10.7% and 28.6% in our image distance and image grating experiments, respectively. These discrepancies can be attributed to the fact that measured data was taken by hand with a millimeter ruler, so human error likely affected our results. If this lab were to be repeated in the future, it would be beneficial to mitigate human error by employing a computerized method of measuring length.